Acoustic phonon generation from quasi-2D hole gas in quantum wells

2001 J. Phys.: Condens. Matter 13 10851

(http://iopscience.iop.org/0953-8984/13/48/311)

INSTITUTE OF PHYSICS PUBLISHING JOURNAL OF PHYSICS: CONDENSED MATTER

J. Phys.: Condens. Matter **13** (2001) 10851–10863 PII: S0953-8984(01)21709-3

Acoustic phonon generation from quasi-2D hole gas in quantum wells

I-K Oh and Jai Singh

Faculty of SITE B28, Northern Territory University, Darwin, NT 0909, Australia

Received 7 February 2001, in final form 20 August 2001
Published 16 November 2001
Online at stacks.iop.org/JPhysCM/13/10851

Abstract

The angular and polarization dependences of acoustic phonon emission from a quasi-2D hole gas in quantum wells are theoretically investigated. The contribution of both deformation potential and piezoelectric coupling is considered in the hole–phonon interaction. We have also taken into account the effect of anisotropy of the valence band which gives rise to the hole–phonon interaction due to deformation potential coupling for both LA and TA phonons. Finally, the theory is applied to calculate the rates of acoustic phonon emission in GaAs quantum wells.

1. Introduction

The carrier–phonon interaction in semiconductors plays a very significant role in the performance of their opto-electronic devices. One of the powerful experimental methods to study the effect of carrier–phonon interaction is the phonon spectroscopy using the technique of time-of-flight measurements [1–3], which enables us to investigate the angular and phonon-mode dependences of the charge carrier–phonon interaction, because it is then possible to resolve the emission of longitudinal (LA) and transverse acoustic (TA) phonons. The angular dependence of phonon emission is influenced by several physical factors such as sound waves [4, 5], screening effects [4–6], electronic band structures [7], etc. Within the isotropic model of the sound waves, electron–TA phonon interaction via the deformation potential (DP) vanishes and only LA phonon interaction is non-zero in most III–V cubic semiconductors because the conduction band of such semiconductors near the band minimum is isotropic. In these semiconductors, electrons can interact with both LA and TA phonons only through the piezoelectric (PE) coupling. However, the valence band of most semiconductors near the band maximum is generally anisotropic, which leads to a non-zero hole–acoustic phonon coupling through DP for both LA and TA phonons. As a result, the hole–acoustic phonon interaction becomes non-zero for both LA and TA phonons from DP as well as PE couplings. On the other hand, for elastically anisotropic solids, three types of sound waves can propagate in a given direction and generally none of them is purely longitudinal or transverse (so they are called quasi-longitudinal, fast and slow quasi-transverse waves) except for specific directions such as symmetry axes [8]. Therefore, it is to be noted that for such elastically anisotropic solids, the electrons in the isotropic conduction band can interact with the quasi-TA phonons due to acoustic anisotropy [4, 5] since the direction of the polarization vector for the quasi-TA phonons is not exactly perpendicular to that of the propagation of the quasi-TA phonons.

During the last two decades, a considerable number of experimental [1–3, 9–15] and theoretical [4, 16–20] studies on acoustic phonon emission from 2D electrons have been reported. However, fewer research activities have been devoted to the hole–acoustic phonon interaction in semiconductor nanostructures. Using the current pulses, Strickland *et al* [21] have studied the phonon emission from a hot two-dimensional hole gas (2DHG) in (3 1 1) GaAs/AlGaAs heterojunctions. Their result shows that the phonon emission from a 2DHG in the (3 1 1) GaAs/AlGaAs heterojunction is restricted to angles less than $\theta = 30^\circ$. Recently, Kent *et al* [22, 23] have investigated experimentally the hole–acoustic phonon interaction using the phonon absorption [22] and emission [23] from a 2DHG in GaAs heterojunctions. They have also calculated the phonon absorption [22] and emission [23] as a function of the angle for both LA and TA modes by using an average effective DP constant for both LA and TA modes, i.e. identical and isotropic DP for both LA and TA phonons. More recently, Lehmann *et al* [6] have studied the phonon emission from both 2D electrons and holes in a GaAs heterojunction using the same DP as a parameter for both LA and TA phonons. However, the study of acoustic phonon emission from a 2DHG in GaAs quantum wells (QWs) has not yet been done either experimentally or theoretically. In this paper, we present a comprehensive theory of acoustic phonon emission from a 2DHG in QWs considering both anisotropic DP and PE couplings.

This paper is organized as follows. In section 2, we present the derivation of a Hamiltonian which describes the hole–acoustic phonon interactions due to both DP and PE couplings in QWs. The phonon emission rate from a 2DHG as a function of angles, hole and lattice temperatures, hole density and phonon energy is derived in section 3, and in section 4, the results of the rate of emission in GaAs QWs are presented and their significance is discussed.

2. Hole–acoustic phonon interaction

Strains due to acoustic phonons in non-centrosymmetric semiconductors give rise to a deformation in the bandstructure as well as a change in the macroscopic electric potential energy. The former is related to DP coupling and the latter is related to PE coupling with charge carriers. An electronic transition of charge carriers can also induce strains in such semiconductors via DP and PE couplings. In this section, we derive expressions for the hole–acoustic phonon interactions due to both DP and PE couplings within the isotropic model of acoustic waves where the displacement vector of lattice, i.e. polarization vector, for LA phonons is parallel to the direction of propagation, i.e. wave vector, and that for TA phonons is perpendicular to the wave vector.

The DP energy w of the valence band due to a strain caused by λ-mode (LA, TA_1 or TA_2) acoustic phonons with wave vector $\boldsymbol{q}$ can be written as [24]

$$w(\boldsymbol{r}, t)_{\mathrm{v},\lambda\boldsymbol{q}} = \sum_{ij} \Xi_{ij,\mathrm{v}} u_{ij}(\boldsymbol{r}, t)_{\lambda\boldsymbol{q}} \qquad i, j = 1, 2, 3 \tag{1}$$

where the subscript 'v' denotes the valence band. The strain tensor $u_{ij}(\boldsymbol{r}, t)_{\lambda\boldsymbol{q}}$ due to a single phonon is given by

$$u_{ij}(\boldsymbol{r}, t)_{\lambda\boldsymbol{q}} = \frac{1}{2}\left(\frac{\partial u_i}{\partial x_j} + \frac{\partial u_j}{\partial x_i}\right) \tag{2}$$

where u_i is the ith component of the displacement vector $\boldsymbol{u}(\boldsymbol{r},t)_{\lambda\boldsymbol{q}}$ of the lattice associated with a λ-mode acoustic phonon with wave vector $\boldsymbol{q}$. It can be written in terms of phonon creation and annihilation operators $\hat{b}^{\dagger}_{\lambda\boldsymbol{q}}$ and $\hat{b}_{\lambda\boldsymbol{q}}$, respectively, as [25]

$$\boldsymbol{u}(\boldsymbol{r},t)_{\lambda\boldsymbol{q}} = \sqrt{\frac{\hbar}{2\rho_m v_\lambda q V}}\boldsymbol{d}_{\lambda\boldsymbol{q}}\left(\hat{b}_{\lambda\boldsymbol{q}}\mathrm{e}^{\mathrm{i}(\boldsymbol{q}\cdot\boldsymbol{r}-v_\lambda q t)} + \hat{b}^{\dagger}_{\lambda\boldsymbol{q}}\mathrm{e}^{-\mathrm{i}(\boldsymbol{q}\cdot\boldsymbol{r}-v_\lambda q t)}\right) \tag{3}$$

where ρ_m is the material density, V the volume, v_λ the sound velocity and $\boldsymbol{d}_{\lambda\boldsymbol{q}}$ the polarization vector associated with the λ-mode phonon. Using equations (2) and (3) in equation (1), the DP energy becomes

$$w(\boldsymbol{r},t)_{\mathrm{v},\lambda\boldsymbol{q}} = \mathrm{i}\sqrt{\frac{\hbar q}{2\rho_m v_\lambda V}}\,\Xi^{\lambda}_{\mathrm{v}}(\boldsymbol{q})\left(\hat{b}_{\lambda\boldsymbol{q}}\mathrm{e}^{\mathrm{i}(\boldsymbol{q}\cdot\boldsymbol{r}-v_\lambda q t)} - \mathrm{c.c.}\right) \tag{4}$$

where c.c. stands for complex conjugate and the effective DP constant is given by

$$\Xi^{\lambda}_{\mathrm{v}}(\boldsymbol{q}) = \frac{1}{2}\sum_{ij}\Xi_{ij,\mathrm{v}}\left(d^{i}_{\lambda\boldsymbol{q}}e_j + d^{j}_{\lambda\boldsymbol{q}}e_i\right) \qquad \boldsymbol{e} = \frac{\boldsymbol{q}}{q}. \tag{5}$$

Here $\boldsymbol{e} = (e_1, e_2, e_3)$ is a unit vector in the direction of phonon propagation. The detailed derivation of the effective deformation potentials $\Xi^{\lambda}_{\mathrm{v}}(\boldsymbol{q})$ for each acoustic phonon mode associated with the valence band edge is given in [7].

In non-centrosymmetric crystals such as III–V and II–VI polar semiconductors, a strain associated with the acoustic phonon can induce macroscopic electric polarization in the crystal, which is known as the PE effect. For the cubic crystals of such polar semiconductors, the electric potential $\varphi_{\lambda\boldsymbol{q}}$ due to the PE fields produced by a single λ-mode acoustic phonon with wave vector $\boldsymbol{q}$ can be written as [24]

$$\varphi_{\lambda\boldsymbol{q}} = -\mathrm{i}\frac{\boldsymbol{q}\cdot\boldsymbol{P}_{\lambda\boldsymbol{q}}}{\kappa\epsilon_0 q^2} \tag{6}$$

where $\boldsymbol{P}_{\lambda\boldsymbol{q}}$ is the electric polarization induced by a λ-mode phonon, κ the relative dielectric constant and ϵ_0 the electric permittivity in the vacuum. The ith component of the electric polarization is given by

$$P^{i}_{\lambda\boldsymbol{q}} = \sum_{jk} h_{ijk} u_{jk}(\boldsymbol{r},t)_{\lambda\boldsymbol{q}} \tag{7}$$

where h_{ijk} is the PE tensor. Using equations (2) and (7) in equation (6), we get the electric potential energy $U_{\lambda\boldsymbol{q}}$ for a charge carrier with electric charge Q as

$$U_{\lambda\boldsymbol{q}} = Q\varphi_{\lambda\boldsymbol{q}} = \left(\frac{Qh^{\lambda}_{\boldsymbol{q}}}{\kappa\epsilon_0}\right)\sqrt{\frac{\hbar}{2\rho_m v_\lambda q V}}\left(\hat{b}_{\lambda\boldsymbol{q}}\mathrm{e}^{\mathrm{i}(\boldsymbol{q}\cdot\boldsymbol{r}-v_\lambda q t)} - \mathrm{c.c.}\right) \tag{8}$$

where $h^{\lambda}_{\boldsymbol{q}}$ is the effective PE constant for a λ-mode phonon given by

$$h^{\lambda}_{\boldsymbol{q}} = \frac{1}{2}\sum_{ijk} h_{ijk}e_i\left(d^{j}_{\lambda\boldsymbol{q}}e_k + d^{k}_{\lambda\boldsymbol{q}}e_j\right). \tag{9}$$

A detailed derivation of the effective PE tensor $h^{\lambda}_{\boldsymbol{q}}$ in the cubic III–V and II–VI semiconductors for both LA and TA phonons is given in [7]. It is to be noted that a comparison of the expression of the potential in equation (4) and that of the PE potential in equation (8) reveals that there exists a critical λ-mode phonon wave vector q_0 given by

$$q_0 = \frac{1}{\kappa\epsilon_0}\left(\frac{Qh^{\lambda}_{\boldsymbol{q}}}{\Xi^{\lambda}_{\mathrm{v}}(\boldsymbol{q})}\right) \tag{10}$$

such that for phonons with wave vector $q < q_0$, the PE coupling is dominant and for $q > q_0$ the DP coupling is dominant for a given charge carrier and a given direction of phonon propagation.

Using the expressions for the two types of hole–phonon interactions as described above, we can get the corresponding hole–phonon interaction Hamiltonians $H^I_{h-p,\lambda}$ due to DP ($I = D$) and PE coupling ($I = P$) as

$$H^I_{h-p}(\boldsymbol{r})_{\lambda,\boldsymbol{q}} = g^\lambda_I(\boldsymbol{q})\mathrm{e}^{\mathrm{i}\boldsymbol{q}\cdot\boldsymbol{r}}\hat{b}_{\lambda\boldsymbol{q}} + \text{c.c.} \tag{11}$$

where

$$g^\lambda_D(\boldsymbol{q}) = -\mathrm{i}\sqrt{\frac{\hbar q}{2\rho_m v_\lambda V}}\,\Xi^\lambda_{\mathrm{v}}(\boldsymbol{q}) \tag{12}$$

$$g^\lambda_P(\boldsymbol{q}) = \sqrt{\frac{\hbar}{2\rho_m v_\lambda q V}}\left(\frac{eh^\lambda_{\boldsymbol{q}}}{\kappa\epsilon_0}\right). \tag{13}$$

Introducing the creation (annihilation) operators $\hat{c}^\dagger_{n,\boldsymbol{k}_\parallel}$ ($\hat{c}_{n,\boldsymbol{k}_\parallel}$) of a hole in the nth subband of QWs with the wave vector $\boldsymbol{k}_\parallel$, the field operator $\hat{\psi}$ for holes can be written as

$$\hat{\psi}(\boldsymbol{r}_\parallel, z) = \frac{1}{\sqrt{A_0}}\sum_{n,\boldsymbol{k}_\parallel}\mathrm{e}^{\mathrm{i}\boldsymbol{k}_\parallel\cdot\boldsymbol{r}_\parallel}\phi_n(z)\hat{c}_{n,\boldsymbol{k}_\parallel} \tag{14}$$

where A_0 is the 2D area of quantum wells and $\phi_n(z)$ is the hole wave function for the nth bound state for the hole motion along the z-axis which is assumed to be perpendicular to the wall of quantum wells. Using equations (11) and (14), we obtain the hole–phonon interaction Hamiltonian in the second quantized form as

$$\hat{H}^I_{h-p,\lambda} = \int \mathrm{d}\boldsymbol{r}_\parallel \int \mathrm{d}z\,\hat{\psi}^\dagger H^I_{h-p,\lambda}\hat{\psi} = \sum_{\boldsymbol{k}_\parallel,n,n'}\Big[g^\lambda_I(\boldsymbol{q})F_{n,n'}(q_z)\hat{b}_{\lambda\boldsymbol{q}}\hat{c}^\dagger_{n',\boldsymbol{k}_\parallel+\boldsymbol{q}_\parallel}\hat{c}_{n,\boldsymbol{k}_\parallel} + g^{\lambda*}_I(\boldsymbol{q})F^*_{n,n'}(q_z)\hat{b}^\dagger_{\lambda\boldsymbol{q}}\hat{c}^\dagger_{n',\boldsymbol{k}_\parallel-\boldsymbol{q}_\parallel}\hat{c}_{n,\boldsymbol{k}_\parallel}\Big] \tag{15}$$

where the form factor $F_{n,n'}(q_z)$ is obtained as

$$F_{n,n'}(q_z) = \int \mathrm{d}z\,\phi^*_{n'}(z)\phi_n(z)\mathrm{e}^{\mathrm{i}q_z z}. \tag{16}$$

3. Phonon emission rate

The rates of transitions of a hole from an initial state to a final state involving emission or absorption of a single phonon are derived. We represent the initial state by $|i\rangle$ and the final state by $|f\rangle$ as

$$|i\rangle = |\ldots, f^h_{n,\boldsymbol{k}_\parallel}, \ldots, f^h_{n,\boldsymbol{k}_\parallel\mp\boldsymbol{q}_\parallel}, \ldots\rangle|\ldots, n^\lambda_{\boldsymbol{q}}, \ldots\rangle \tag{17}$$

and

$$|f\rangle = |\ldots, f^h_{n',\boldsymbol{k}_\parallel} - 1, \ldots, f^h_{n',\boldsymbol{k}_\parallel\mp\boldsymbol{q}_\parallel} + 1, \ldots\rangle|\ldots, n^\lambda_{\boldsymbol{q}} \pm 1, \ldots\rangle \tag{18}$$

where $f^h_{n,\boldsymbol{k}_\parallel}$ is the occupation number of the nth hole state with wave vector $\boldsymbol{k}_\parallel$ and $n^\lambda_{\boldsymbol{q}}$ is that of a phonon state with wave vector $\boldsymbol{q}$. The upper (lower) sign corresponds to a phonon emission (absorption) process. Using equations (15), (17) and (18), we can get the transition matrix element of phonon emission and absorption as

$$M_{\pm}^{I,\lambda}(n,\boldsymbol{k}_\parallel \to n',\boldsymbol{k}_\parallel \mp \boldsymbol{q}_\parallel; q_z) = \langle f|\hat{H}^{I}_{h-p,\lambda}(\boldsymbol{q}_\parallel, q_z)|i\rangle = \mathcal{F}^{I}_{\lambda\pm}(n,n';\boldsymbol{q}_\parallel,q_z) \times \sqrt{\left(1 - f^{h}_{n',\boldsymbol{k}_\parallel \mp \boldsymbol{q}_\parallel}\right) f^{h}_{n,\boldsymbol{k}_\parallel}\left(n^{\lambda}_{\boldsymbol{q}} + \tfrac{1}{2} \pm \tfrac{1}{2}\right)} \tag{19}$$

where

$$\mathcal{F}^{I}_{\lambda-}(n,n';\boldsymbol{q}_\parallel,q_z) = \mathcal{F}^{I*}_{\lambda+}(n,n';\boldsymbol{q}_\parallel,q_z) = g^{\lambda}_{I}(\boldsymbol{q})F_{n,n'}(q_z).$$

We assume that the 2D hole gas and phonon systems are separately in their own thermal equilibrium before the transition. Thus $f^{h}_{n,\boldsymbol{k}_\parallel}$ can be replaced by the average value obtained from the Fermi–Dirac distribution as

$$f^{h}_{n,\boldsymbol{k}_\parallel} = \left[\mathrm{e}^{[E_n(\boldsymbol{k}_\parallel)-\mu]/k_B T_h} + 1\right]^{-1} \tag{20}$$

with

$$E_n(\boldsymbol{k}_\parallel) = \varepsilon_n + \frac{\hbar^2 k_\parallel^2}{2m^{*}_{h\parallel}(\boldsymbol{k}_\parallel, L_z)}$$

where μ is the chemical potential of 2D holes, T_h the hole temperature, ε_n the hole energy in the nth subband and $m^{*}_{h\parallel}(\boldsymbol{k}_\parallel, L_z)$ the in-plane hole effective mass. It is to be noted that the in-plane band structure of a hole in QWs is anisotropic, non-parabolic, complicated and dependent on the well width L_z and it can only be determined numerically [26].

Likewise, $n^{\lambda}_{\boldsymbol{q}}$ can be replaced by the average value obtained from the Bose–Einstein distribution as

$$n^{\lambda}_{\boldsymbol{q}} = \left[\mathrm{e}^{\hbar\omega_{\boldsymbol{q},\lambda}/k_B T} - 1\right]^{-1} \tag{21}$$

where T is the lattice temperature.

Applying the Fermi golden rule and using the transition matrix elements in equation (19), the rate of such transition with emission or absorption of a λ-mode phonon of wave vector $\boldsymbol{q}$ can be written as

$$W_{\pm}^{I,\lambda}(n,\boldsymbol{k}_\parallel \to n',\boldsymbol{k}_\parallel \mp \boldsymbol{q}_\parallel; q_z) = \frac{2\pi}{\hbar}\left|M_{\pm}^{I,\lambda}(n,\boldsymbol{k}_\parallel \to n',\boldsymbol{k}_\parallel \mp \boldsymbol{q}_\parallel; q_z)\right|^2 \times \delta(E_{n'}(\boldsymbol{k}_\parallel \mp \boldsymbol{q}_\parallel) - E_n(\boldsymbol{k}_\parallel) \pm \hbar\omega_{\boldsymbol{q},\lambda}). \tag{22}$$

Using equation (19) in (22), we get

$$W_{\pm}^{I,\lambda}(n,\boldsymbol{k}_\parallel \to n',\boldsymbol{k}_\parallel \mp \boldsymbol{q}_\parallel; q_z) = \frac{2\pi}{\hbar}\left|\mathcal{F}^{I}_{\lambda\pm}(n,n';\boldsymbol{q}_\parallel,q_z)\right|^2\left(1 - f^{h}_{n',\boldsymbol{k}_\parallel \mp \boldsymbol{q}_\parallel}\right) f^{h}_{n,\boldsymbol{k}_\parallel} \times \left(n^{\lambda}_{\boldsymbol{q}} + \frac{1}{2} \pm \frac{1}{2}\right)\delta(E_{n'}(\boldsymbol{k}_\parallel \mp \boldsymbol{q}_\parallel) - E_n(\boldsymbol{k}_\parallel) \pm \hbar\omega_{\boldsymbol{q},\lambda}). \tag{23}$$

The total scattering rate for a hole with wave vector $\boldsymbol{k}_\parallel$ in the nth subband due to emission (absorption) of a phonon is then obtained by summing over all $\boldsymbol{q}_\parallel$ and q_z in equation (23) as

$$W_{\pm}^{I,\lambda}(n,\boldsymbol{k}_\parallel) = \sum_{n',\boldsymbol{q}_\parallel,q_z} W_{\pm}^{I,\lambda}(n,\boldsymbol{k}_\parallel \to n',\boldsymbol{k}_\parallel \mp \boldsymbol{q}_\parallel; q_z). \tag{24}$$

Equation (23) can be used to study the total phonon emission from all the processes of hole relaxation as the functions of phonon wave vector $\boldsymbol{q}$, hole density and hole temperature.

Taking into account the reverse transition processes involving phonon emission, the net phonon emission rate of a λ-mode phonon with wave vector $\boldsymbol{q}$ can be written as

$$\frac{\partial n_{\boldsymbol{q}}^{\lambda}}{\partial t} = \sum_{n,n',I,\boldsymbol{k}_\parallel} \mathcal{W}_{\lambda}^{I}(n,n';\boldsymbol{q}_\parallel,q_z)\left\{\left[\left(1-f^{h}_{n',\boldsymbol{k}_\parallel-\boldsymbol{q}_\parallel}\right)f^{h}_{n,\boldsymbol{k}_\parallel}\left(n_{\boldsymbol{q}}^{\lambda}+1\right)\right.\right.$$
$$\left. -\left(1-f^{h}_{n',\boldsymbol{k}_\parallel}\right)f^{h}_{n,\boldsymbol{k}_\parallel-\boldsymbol{q}_\parallel}n_{\boldsymbol{q}}^{\lambda}\right]\delta(E_{n'}(\boldsymbol{k}_\parallel-\boldsymbol{q}_\parallel)-E_n(\boldsymbol{k}_\parallel)+\hbar\omega_{\boldsymbol{q},\lambda})$$
$$-\left[\left(1-f^{h}_{n',\boldsymbol{k}_\parallel+\boldsymbol{q}_\parallel}\right)f^{h}_{n,\boldsymbol{k}_\parallel}n_{\boldsymbol{q}}^{\lambda}-\left(1-f^{h}_{n',\boldsymbol{k}_\parallel}\right)f^{h}_{n,\boldsymbol{k}_\parallel+\boldsymbol{q}_\parallel}\left(n_{\boldsymbol{q}}^{\lambda}+1\right)\right]$$
$$\left.\times\,\delta(E_{n'}(\boldsymbol{k}_\parallel+\boldsymbol{q}_\parallel)-E_n(\boldsymbol{k}_\parallel)-\hbar\omega_{\boldsymbol{q},\lambda})\right\} \qquad (25)$$

where

$$\mathcal{W}_{\lambda}^{I}(n,n';\boldsymbol{q}_\parallel,q_z)=\frac{2\pi}{\hbar}\left|\mathcal{F}_{\lambda+}^{I}(n,n';\boldsymbol{q}_\parallel,q_z)\right|^2=\frac{2\pi}{\hbar}\left|\mathcal{F}_{\lambda-}^{I}(n,n';\boldsymbol{q}_\parallel,q_z)\right|^2. \qquad (26)$$

Using equation (25) the rates of phonon emission are calculated numerically as a function of phonon wave vector, hole density and hole temperature as presented in the next section.

4. Results and discussion

We have presented a theory to calculate the rate of phonon emission due to the processes of hole relaxation in QWs. In studying the acoustic phonon emission from a 2DHG in GaAs QWs, one needs to consider the anisotropies of sound waves, effective mass and coupling constants. Here we have focused only on the effect of anisotropy in coupling constants of DP and PE interactions. Therefore, we have used isotropic sound waves and hole effective masses, i.e., $v_{\mathrm{TA}_1}(\boldsymbol{e}) = v_{\mathrm{TA}_2}(\boldsymbol{e}) = v_{\mathrm{TA}}$, $v_{\mathrm{LA}}(\boldsymbol{e}) = v_{\mathrm{LA}}$ and $m^*_{h\parallel}(\boldsymbol{k}_\parallel, L_z) = m^*_{h\parallel}$ in the calculation presented in this paper for [0 0 1] GaAs/$\mathrm{Al}_x\mathrm{Ga}_{1-x}$As QWs to calculate the rate of phonon emission as a function of the angles of phonon emission (θ and ϕ), hole temperature (T_h) and density (n_h), phonon energy (E_{ph}) and QW width (L_z). The material parameters used in the calculation for GaAs QWs are as follows: effective masses of heavy holes [27] $m^*_{h\parallel} = 0.11m_e$ ($m_e = 9.10953\times10^{-31}$ kg), $m^*_{h\perp} = 0.33m_e$, DPs of valence band [28], $l = -2.24$ eV, $m = 2.86$ eV, $n = -7.88$ eV, relative dielectric constant $\kappa = 12.9$ [27], PE constant $h_{14} = -0.16$ C m^{-2} [27], material density $\rho_m = 5.3175\times10^3$ kg m^2 [27], sound velocity for LA mode $v_{\mathrm{LA}} = 5.29\times10^5$ cm s^{-1} [27], sound velocity for TA mode $v_{\mathrm{TA}} = 2.48\times10^5$ cm s^{-1} [27] and lattice temperature $T = 4.2$ K.

Experimentally, the density n_h of a 2DHG can be adjusted by changing the p-type doping density and its temperature T_h can be controlled by changing the strength of the current pulses [22, 29]. The angular and mode dependencies of phonon emission can be measured by an appropriate configuration of a superconducting bolometer (Pb or Al bolometer) [2]. The phonon energy dependence of acoustic phonon emission can also be studied by using the superconducting bolometers since a Pb bolometer acts as a narrow-band detector (approximately 650–800 GHz) and an Al bolometer behaves as a broad-band detector (approximately 100–800 GHz) [2].

The theory developed in the previous section is general and can be applied for both inter- and intra-subband transitions. However, here we have calculated the rates of acoustic phonon emission only through the intra-subband transitions within the first subband for QWs of width $L_z = 10-160$ Å and using the valence-band discontinuity $\Delta E_v(x) = 0.17x$ eV [27] at $x = 0.3$. The numerical calculations producing the results shown in figures 1–6 are made for a narrow QW of width $L_z = 28$ Å where only one hole subband exists and therefore no inter-subband transitions can take place. Our results reveal that there is only one subband in

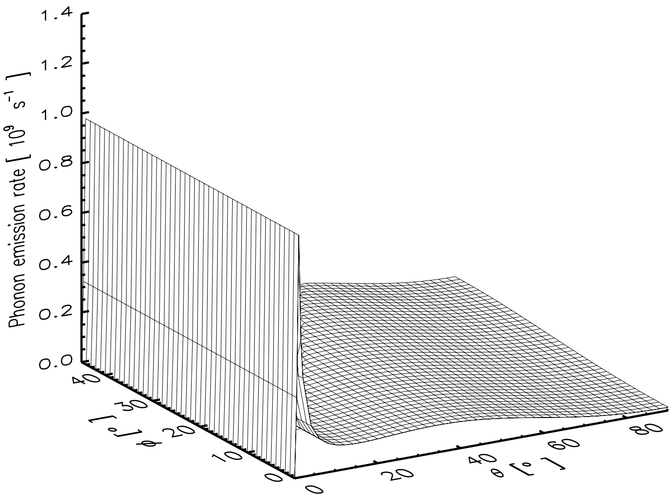

Figure 1. LA phonon emission rate due to DP coupling plotted as a function of phonon emission angles (θ, ϕ) for GaAs/$Al_{0.3}Ga_{0.7}As$ QWs with well width $L_z = 28$ Å, phonon energy $E_{ph} = 0.1$ meV, hole density $n_h = 3 \times 10^{11}$ cm^{-2}, hole temperature $T_h = 15$ K and lattice temperature $T = 4.2$ K.

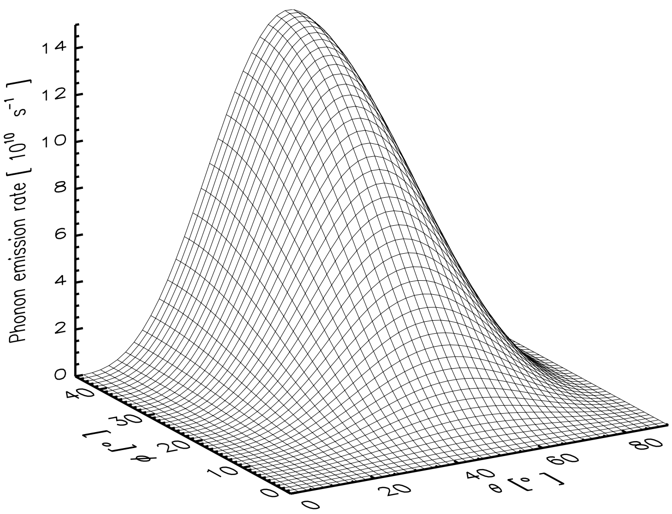

Figure 2. LA phonon emission rate due to PE coupling plotted as a function of phonon emission angles (θ, ϕ) for GaAs/$Al_{0.3}Ga_{0.7}As$ QWs with well width $L_z = 28$ Å, phonon energy $E_{ph} = 0.1$ meV, hole density $n_h = 3 \times 10^{11}$ cm^{-2}, hole temperature $T_h = 15$ K and lattice temperature $T = 4.2$ K.

QWs of widths 10–47 Å, there are two subbands in QWs of widths 48–94 Å, three in widths 95–141 Å and four in widths 142–160 Å. In QWs of widths 48–160 Å, the energy separation $\Delta\epsilon_{12}$ between the first and second subbands ranges from $\Delta\epsilon_{12} = 34$ meV (in $L_z = 48$ Å) to 9 meV (in $L_z = 160$ Å). Thus, even the lowest energy separation of 9 meV in QWs of 160 Å is much larger than the Fermi energy of 3.27 meV at $T_h = 0$ K and a hole density of $n_h = 1.5 \times 10^{11}$ cm^{-2}. Therefore, at such a low hole density ($n_h = 1.5 \times 10^{11}$ cm^{-2}) and temperature ($T_h = 15$ K), although acoustic phonon emission may occur due to both intra- and inter-subband

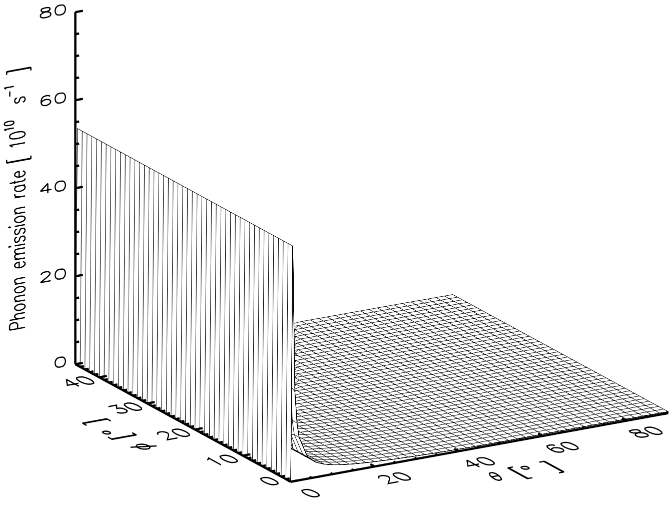

Figure 3. TA phonon emission rate due to DP coupling plotted as a function of phonon emission angles (θ, ϕ) for GaAs/$Al_{0.3}Ga_{0.7}As$ QWs with well width $L_z = 28$ Å, phonon energy $E_{ph} = 0.1$ meV, hole density $n_h = 3 \times 10^{11}$ cm^{-2}, hole temperature $T_h = 15$ K and lattice temperature $T = 4.2$ K.

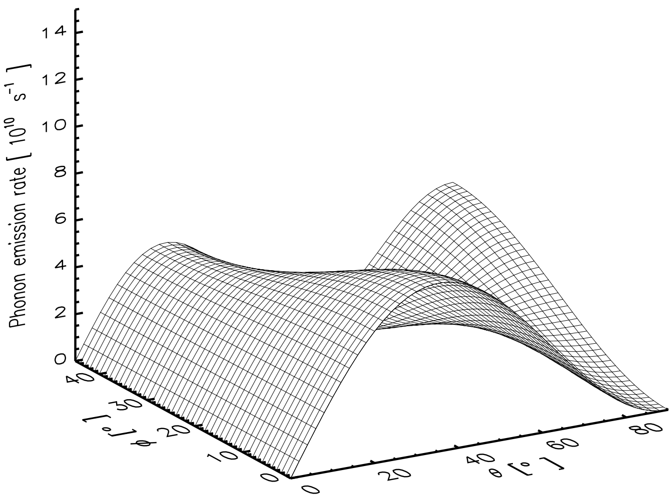

Figure 4. TA phonon emission rate due to PE coupling plotted as a function of phonon emission angles (θ, ϕ) for GaAs/$Al_{0.3}Ga_{0.7}As$ QWs with well width $L_z = 28$ Å, phonon energy $E_{ph} = 0.1$ meV, hole density $n_h = 3 \times 10^{11}$ cm^{-2}, hole temperature $T_h = 15$ K and lattice temperature $T = 4.2$ K.

transitions, the contribution of the inter- and intra-subband transitions in higher subbands is expected to be relatively very small and can be neglected. The results shown in figure 7 are thus obtained by applying this condition. However, for higher densities and temperatures of 2DHG in QWs of wider widths, possibly 200 Å or more, inter-subband transitions involving acoustic phonon emission may become important. In QWs of narrow widths, only LO phonon emission may be dominant through inter-subband transitions at higher hole densities and temperatures. However, LO phonon emission is not considered in this paper. Therefore, the

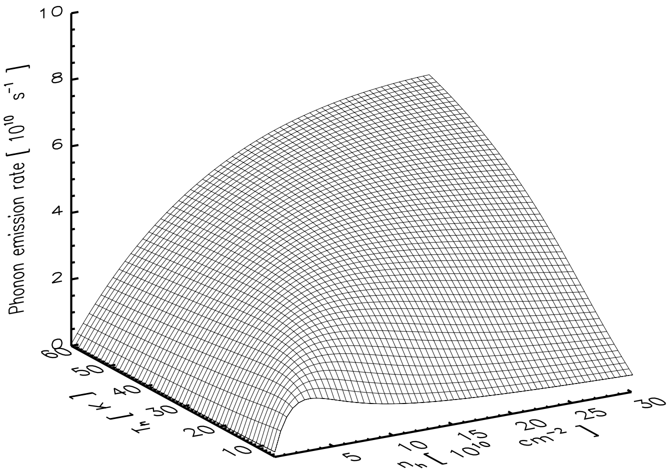

Figure 5. Rate of acoustic phonon emission due to both DP and PE couplings plotted as a function of density (n_h) and temperature (T_h) of 2DHG for GaAs/$Al_{0.3}Ga_{0.7}As$ QWs with well width $L_z = 28$ Å, phonon energy $E_{ph} = 1.0$ meV, $\theta = 5°$, $\phi = 25°$, and lattice temperature $T = 4.2$ K.

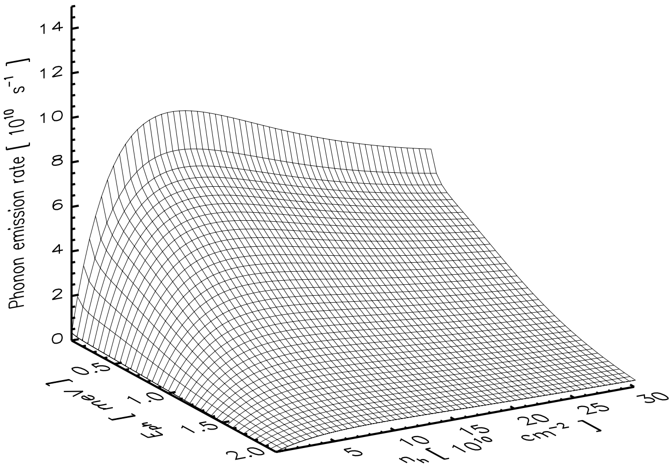

Figure 6. Rate of acoustic phonon emission due to both DP and PE couplings plotted as a function of hole density (n_h) and phonon energy (E_{ph}) for GaAs/$Al_{0.3}Ga_{0.7}As$ QWs with well width $L_z = 28$ Å, $\theta = 5°$, $\phi = 25°$, hole temperature $T_h = 15$ K and lattice temperature $T = 4.2$ K.

neglect of inter-subband transitions at low hole densities and temperatures as considered here is fully justified for acoustic phonon emission.

It may be considered desirable here to discuss the assumption of separate states of equilibrium for holes and phonons as considered in the theory presented in section 3. It is possible to maintain the crystal at a temperature by mounting the sample in a helium cryostat and heat 2DHG (or 2DEG) by passing current pulses [22, 29] to any higher temperature different from the lattice temperature. Since the thermalization of holes is quicker than that of phonons, one can assume, as an initial condition, that holes and phonons are separately in

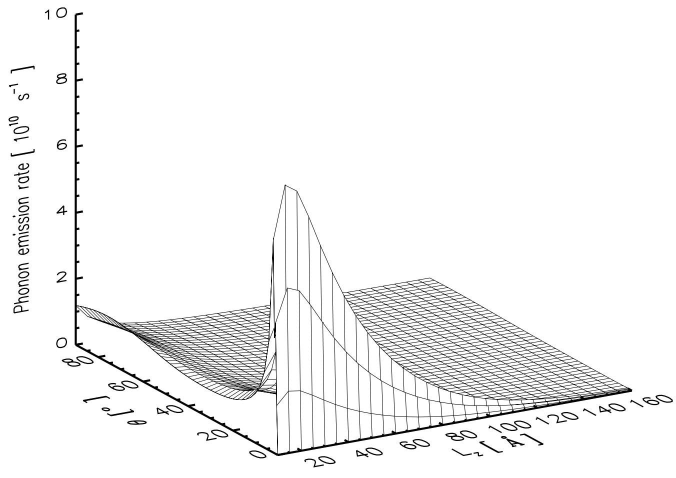

Figure 7. Rate of acoustic phonon emission due to both DP and PE couplings plotted as a function of well width (L_z) and angle θ for GaAs/$Al_{0.3}Ga_{0.7}As$ QWs with phonon energy $E_{ph} = 1.0$ meV, $\phi = 25^\circ$, hole density $n_h = 1.5 \times 10^{11}$ cm^{-2}, hole temperature $T_h = 15$ K and lattice temperature $T = 4.2$ K.

their own thermal equilibrium but not in thermal equilibrium with each other. Thus holes can be set initially in thermal equilibrium at a temperature T_h higher than the temperature of the thermal equilibrium of the lattice.

Using the phonon energy $E_{ph} = 0.1$ meV, lattice temperature $T = 4.2$ K, hole density $n_h = 3 \times 10^{11}$ cm^{-2} and hole temperature $T_h = 15$ K, we have plotted in figure 1 the rate of LA phonon emission from a 2DHG due to DP coupling for $L_z = 28$ Å QWs as a function of the angles θ and ϕ in the spherical coordinate system with the z-axis perpendicular to the QW plane. The result shows that the rate of LA phonon emission is very sensitive to the angle θ but it is almost independent of the angle ϕ. This trend is very similar to the result of LA phonon emission from a 2DEG calculated using an electron–phonon interaction without the screening effect and without phonon focusing [5]. A peak rate of 9.8×10^8 s^{-1} occurs at $\theta = 1^\circ$ in a direction nearly parallel to the z-axis, and another small peak value of 1.7×10^8 s^{-1} is found to occur at $\theta = 40^\circ$. As the phonon energy increases, the first peak rate reduces rapidly but the angle $\theta = 1^\circ$ at which the peak rate occurs, remains unchanged. However, the second peak rate decreases very slowly and its angular position shifts first towards a larger angle θ and then a smaller angle θ. These results are given in table 1, which shows that at larger phonon energies both peak rates become comparable. For example, the first peak rate of phonon emission due to DP coupling at the phonon energy of $E_{ph} = 0.1$ meV is 9.8×10^8 s^{-1} and it occurs at $\theta = 1^\circ$, and the second peak rate of 1.7×10^8 s^{-1} occurs at $\theta = 40^\circ$. At $E_{ph} = 2.5$ meV, the first peak rate reduces to 2.1×10^8 s^{-1} still occurring at $\theta = 1^\circ$ and the second peak rate of 1.4×10^8 s^{-1} occurs at $\theta = 62^\circ$. Then at $E_{ph} = 3.0$ meV, the first peak rate of 1.2×10^8 s^{-1} occurs at $\theta = 1^\circ$ and the second peak rate becomes 1.0×10^8 s^{-1} at $\theta = 54^\circ$. A comparison of our results with the previous theoretical results [5] for phonon emission from a 2DEG may imply that the occurrence of the first peak is due to the exclusion of the screening effect. However, as the intensity of the first peak reduces with increase in phonon energy, it is difficult to compare the two results directly. First, because in the present paper we have focused primarily on the effect of anisotropy in the valence band and not on the screening effect. In the previous paper by Lehmann and Jasiukiewicz [5], the effect of screening on phonon emission due to electron–phonon interaction in the conduction band was studied. Moreover, as emission was integrated over the phonon energy, the dependence of emission on phonon energy could not be assessed [5]. It may also be pointed out here that the screening effect for holes is quite different from that of electrons. Therefore, a direct comparison may not be possible without considering the screening effect on phonon emission from a 2DHG.

Table 1. Peak rates and the corresponding angle θ for LA phonon emission due to DP and PE coupling calculated at different phonon energies E_{ph}.

	DP				PE	
E_{ph} (meV)	First peak value (s^{-1})	θ (°)	Second peak value (s^{-1})	θ (°)	Maximum value (s^{-1})	θ (°)
0.1	9.8×10^8	1	1.7×10^8	40	1.4×10^{11}	51
1.0	7.3×10^8	1	1.5×10^8	45	1.3×10^9	53
1.7	4.4×10^8	1	1.4×10^8	54	4.3×10^8	56
2.5	2.1×10^8	1	1.4×10^8	62	2.0×10^8	60
3.0	1.2×10^8	1	1.0×10^8	54	1.0×10^8	55
3.5	6.8×10^7	1	5.6×10^7	45	3.7×10^7	47

Using the same lattice temperature, hole density, hole temperature and QW width as used for calculating the rates shown in figure 1, we have plotted the rate of LA phonon emission due to PE coupling in figure 2 at a phonon energy $E_{ph} = 0.1$ meV. Unlike the rate of LA phonon emission due to DP coupling, the rate of phonon emission due to PE coupling is very sensitive to both the angles θ and ϕ and it has only one peak value. The maximum rate of phonon emission due to PE coupling is 1.40×10^{11} s^{-1} at $\theta = 52°$ and $\phi = 45°$ which is about three orders of magnitude higher than the maximum rate due to DP coupling shown in figure 1. This means that the rate of LA phonon emission at the low phonon energy of $E_{ph} = 0.1$ meV is dominated by PE interaction. The maximum rates of phonon emission due to PE coupling at different phonon energies are also tabulated in table 1 along with their angles. According to table 1, the maximum rate of phonon emission at different phonon energies occurs at different angles. This behaviour is similar to the second peak rate obtained through DP coupling. For example, the maximum rate of phonon emission due to PE coupling at the phonon energy of $E_{ph} = 0.1$ meV is 1.4×10^{11} s^{-1} and it occurs at $\theta = 53°$, at $E_{ph} = 2.5$ meV, the maximum rate of 2.0×10^8 s^{-1} occurs at $\theta = 60°$ and at $E_{ph} = 3.0$ meV, the maximum rate of 1.0×10^8 s^{-1} occurs at $\theta = 55°$. As far as the maximum rate of LA phonon emission is concerned, our calculation shows that the emission rate is dominated by PE coupling for phonon energies $E_{ph} \lesssim 1.7$ meV and by DP coupling for $E_{ph} \gtrsim 1.7$ meV.

Figures 3 and 4 show the rate of TA phonon emission calculated as a function of phonon emission angles due to DP and PE couplings, respectively. The material parameters and the conditions of configuration for QWs are the same as those in figure 1. The θ angle dependence of phonon emission due DP coupling is similar to that in figure 1, but the maximum rate of TA phonon emission is 5.3×10^{11} s^{-1} at $\theta = 0.5°$ which is much larger than that of LA phonon emission due to DP. This means that the phonon emission near $\theta = 0°$ is dominated by the TA phonon through DP coupling. The rate of TA phonon emission due to PE coupling is very sensitive to both θ and ϕ angles (see figure 4). There are three peaks: (1) the first peak value of 4.3×10^{10} s^{-1} at $\theta = 22°$ and $\phi = 45°$ and the second 4.7×10^{10} s^{-1} at $\theta = 90°$ and $\phi = 45°$ are due to TA_1 phonons; (2) the third peak value of 7.2×10^{10} s^{-1} at $\theta = 36°$ and

$\phi = 0^\circ$ corresponds to TA_2 phonon. Here also the peak value rates decrease as the phonon energy increases.

We have plotted the rate of acoustic phonon (i.e. LA + TA) emission in figure 5 as a function of the hole density n_h and hole temperature T_h for a 2DHG with the following conditions: $T_h = 5$–60 K, $n_h = (0.1$–$30) \times 10^{10}$ cm^{-2}, $L_z = 28$ Å, $E_{\rm ph} = 1.0$ meV, $\theta = 5^\circ$, $\phi = 25^\circ$ and $T = 4.2$ K. At a given temperature of 2DHG, phonon emission increases to a peak value and then decreases with increasing density of 2DHG. At higher temperatures, the peak value occurs at higher densities n_h (see figure 5). For example, the peak rate for $T_h =$ 10 K occurs at $n_h \sim 5.6 \times 10^{10}$ cm^{-2} and for $T_h = 20$ K it is at $n_h \sim 1.1 \times 10^{11}$ cm^{-2}. This information is very important for designing a ultrasonic generator device using QWs to be able to control the density of 2DHG through controlling p-type doping density and the temperature of 2DHG by the current pulse.

Figure 6 shows the rate of acoustic phonon emission as a function of density n_h of 2DHG and phonon energy $E_{\rm ph}$. We have used the following values in the calculation: $n_h = (0.1$–$30) \times 10^{10}$ cm^{-2}, $E_{\rm ph} = 0.1$–2 meV, $L_z = 28$ Å, $\theta = 5^\circ$, $\phi = 25^\circ$, $T_h = 15$ K and $T = 4.2$ K. It is found that first the phonon emission increases rapidly to a maximum value and then it decreases very slowly with increasing the density of 2DHG. The maximum rate of acoustic phonon emission occurs at $n_h \sim 4.6 \times 10^{10}$ cm^{-2} and does not change with $E_{\rm ph}$. Therefore, it is suggested that the p-type doping should be controlled such that the value of $n_h \sim 4.6 \times 10^{10}$ cm^{-2} in order to get the maximum acoustic phonon generation for the above configurations of QWs.

Finally, we have plotted in figure 7 the rate of acoustic phonon emission as a function of width L_z of QWs and emission angle θ using the following values: $L_z = 10-160$ Å, $\theta = 0-90^\circ$, $E_{\rm ph} = 1.0$ meV, $\phi = 25^\circ$, $n_h = 1.5 \times 10^{11}$ cm^{-2}, $T_h = 15$ K and $T = 4.2$ K. Maximum phonon emission can be achieved at $L_z = 15$ Å for $\theta \lesssim 42^\circ$. For $\theta \gtrsim 42^\circ$, the rate of acoustic phonon emission decreases as the width of QWs increases.

In summary, we have presented a comprehensive theory to calculate the rate of acoustic phonon emission from a 2DHG in QWs as a function of phonon emission angles, phonon energy, phonon mode, width of QWs and density and temperature of 2DHG. Our results show that TA phonon emission via DP coupling is dominant at smaller θ angles over the other processes. We have found that the rate of acoustic phonon emission is very sensitive to phonon energy, density of 2DHG and width of QWs. It is expected that the present results will be found to be very useful in designing ultrasonic generators using QWs and in enhancing our understanding of the hole scattering processes through acoustic phonons in QWs.

Acknowledgments

This work was supported by an Australian Research Council's large grants scheme.

References

[1] Chin M A, Narayanamurti V, Stormer H L and Hwang J C M 1984 *Phonon Scattering in Condensed Matter* ed W Eisenmenger, K Laβmann and S Döttinger *Springer Series in Solid-State Sciences* vol 51 (Berlin: Springer)
[2] Rothenfusser M, Köster L and Dietsche W 1986 *Phys. Rev.* B **34** 5518
[3] Challis L J, Toombs G A and Sheard F W 1987 *Physics of Phonons* ed T Paszkiewicz *Lecture Notes in Physics* vol 285 (Berlin: Springer)
[4] Jasiukiewicz C, Lehmann D, Kent A J, Cross A J and Hawker P 1999 *Physca* B **263–264** 183
[5] Lehmann D and Jasiukiewicz C 1999 *Turk. J. Phys.* **23** 583
[6] Lehmann D, Jasiukiewicz C and Kent A J 1998 *Physica* B **249-251** 718
[7] Oh I-K and Singh J 2000 *J. Lumin.* **85** 233

[8] Dieulesaint E and Royer D 1980 *Elastic Waves in Solids* (Chichester: Wiley)
[9] Wigmore J K, Erol M, Sahraoui-Tahar M, Wilkinson C D W, Davies J H and Stanley C 1991 *Semicond. Sci. Technol.* **6** 837
[10] Danilchenko B, Roshko S, Asche M, Hey R, Höricke M and Kostial H 1993 *J. Phys.: Condens. Matter* **5** 3169
[11] Wigmore J K, Erol M, Sahraoui-Tahar M, Ari M, Wilkinson C D W, Davies J H, Holland M and Stanley C 1993 *Semicond. Sci. Technol.* **8** 322
[12] Danilchenko B, Klimashov A, Roshko S, Asche M, Hey R and Kostial H 1994 *J. Phys.: Condens. Matter* **6** 7955
[13] Hawker P, Kent A J, Hauser N and Jagadish C 1995 *Semicond. Sci. Technol.* **10** 601
[14] Kent A J, Cross A, Hawker P and Henini M 1997 *Phys. Status. Solidi* b **204** 230
[15] Cross A J, Kent A J, Hawker P, Lehmann D, Jasiukiewicz C and Henini M 1999 *Physica* B **263–264** 526
[16] Badalian S M and Levinson Y B 1988 *Sov. Phys.–Solid State* **30** 1592
Badalian S M and Levinson Y B 1989 *Phys. Lett.* A **140** 62
Badalian S M and Levinson Y B 1991 *Phys. Lett.* A **155** 200
Badalian S M and Levinson Y B 1992 *Phys. Lett.* A **170** 229
[17] Kitagawa H and Tamura S 1992 *Phys. Rev.* B **46** 4277
[18] Vasko F T, Balev O G and Vasilopoulos P 1993 *Phys. Rev.* B **47** 16 433
Vasko F T and Mitin V V 1995 *Phys. Rev.* B **52** 1500
[19] Xu W and Mahanty J 1994 *J. Phys.: Condens. Matter* **6** 6265
[20] Oh I-K 1996 *PhD Thesis* (Canberra: The Australian National University)
[21] Strickland K R, George R E, Henini M and Kent A J 1994 *Semicond. Sci. Technol.* **9** 786
[22] Kent A J, Strickland R E, Strickland K R and Henini M 1996 *Phys. Rev.* B **54** 2019
[23] Kent A J, Strickland R E, Strickland K R, Cross A J, Hawker P and Henini M 1997 *Semicond. Sci. Technol.* **12** 849
[24] Gantmakher V F and Levinson Y B 1987 *Carrier Scattering in Metals and Semiconductors* (Amsterdam: North-Holland)
[25] Yu P Y and Cardona M 1996 *Fundamentals of Semiconductors: Physics and Materials Properties* (Berlin: Springer)
[26] Bastard G 1988 *Wave Mechanics Applied to Semiconductor Heterostructures* (Les Ulis Cedex: les éditions de physique)
Ridley B K 1997 *Electrons and Phonons in Semiconductor Mutilayers* (Cambridge: Cambridge University Press)
[27] Adachi S 1994 *GaAs and Related Materials: Bulk Semiconducting and Superlattice Properties* (Singapore: World Scientific)
[28] Chuang S L 1995 *Physics of Optoelectronic Devices* (New York: Wiley)
[29] Hawker P, Kent A J, Hughes O H and Challis L J 1992 *Semicond. Sci. Technol.* **7** B 29